JOURNAL OF MECHANICS OF CONTINUA AND MATHEMATICAL SCIENCES
www.journalimcms.org

ISSN (Online) : 2454 -7190 Vol.-19, No.-02, February (2024) pp 79-92 ISSN (Print) 0973-8975

FUNCTIONAL ASSESSMENT OF WAVE PROPAGATION IN IMPERFECT CYLINDER MATERIALS

L. Anitha[1], R. Mehala Devi [2]

Assistant Professor, Department of Mathematics, Nehru Memorial College Puthanampatti, Trichy, Tamilnadu, India;

Assistant Professor, Department of Mathematics, Nandha Arts and Science College Erode, Tamilnadu, India.

E-mail: anithal@nmc.ac.in, mehaladevimaths@gmail.com

Corresponding Author: **R. Mehala Devi**

https://doi.org/10.26782/jmcms.2024.02.00005

(Received: December 14, 2023; Revised: January 20, 2024; Accepted: January 29, 2024)

Abstract

This work provides a theoretical framework to investigate the shear wave propagation properties within an Electrostrictive cylindrical layered structure. The structure is made up of a concentric, Functionally Assessed Electrostrictive Material (FAEM) cylindrical layer of limited width and an inadequately bonded Electrostrictive material cylinder. The FAEM layer has a constant functional gradient in the radial direction, and flaws at the interface are taken seriously, mirroring actual circumstances involving structural and electrical degradation. The fundamental electromechanical connected Bessel's equations are used to simplify field differential equations by mathematical modifications. Relationships for shear wave propagation under electrically short and open circumstances are established analytically. The acquired findings are verified against predefined standards and a particular issue instance. The impact of variables on the phase velocity of shear waves, including functional range and imperfection parameters, is shown through numerical simulations and graphical displays. The research also establishes boundaries for electrically short and open circumstances, taking into account the shear defect that exists between the inner and outer cylindrical layers.

Keywords: Shear Wave Propagation, Cylinder, Electrostrictive Materials, Functional Assessment

I. Introduction

In electromechanical systems, Electrostrictive coupling occurs when electric and displacement fields are linearly linked with mechanical stress and strain [III]. Moreover, the reverse happens: introducing an electric field causes a deformation. Under conditions of mechanical stress, specific crystals form, and an Electrostrictive material will accumulate electrical charges [XIV]; this phenomenon is known as the Electrostrictive effect [VII]. Being reversible implies that materials may display both

the direct and reverse Electrostrictive effects, which is one of the effect's unexpected characteristics.

Because of their special electromechanical qualities, Electrostrictive materials, which are defined by their capacity to deform in response to an applied electric field, have attracted a lot of interest [XIII]. Understanding the behavior of these materials under different situations depends critically on the way shear waves propagate through them [VI]. Electrostrictive materials are useful for actuator and sensor applications because they alter size and form in response to an electric field [II]. To maximize the performance of structures and devices that use these materials, it is essential to comprehend the properties of shear wave propagation [XI]. This paper explores the functional evaluation of shear wave characteristics, taking material composition, frequency, and amplitude into account. This research provides a theoretical framework for using Electrostrictive materials to investigate the properties of Shear Acoustic Wave Propagation (SAWP) inside a cylindrical layered structure. The structure is made up of a concentric arrangement of materials, such as a cylindrical layer of FAEM with restricted breadth and a cylinder of poorly bonded Electrostrictive material. Along the radial direction, the FAEM layer's functional gradient is constant, and interface flaws are considered, mirroring actual situations involving structural and electrical deterioration.

The study is organized as follows: Part 1 explains an Introduction; Part 2 gives a summary of the related works; Part 3 formulates the problem; Part 4 presents an associated solution; and Part 5 deals with boundary conditions. Part 6 presents numerical findings and discussion, while Part 7 provides a summary of the study.

II. Related works

The study [IV] investigated the properties of heat-induced propagation of waves in cylindrical shells using the first-order shear deformation theory of shells, which consists of a metal core layer and two layers of functionally graded material that is insufficient. The shells were responsive to changes in temperature. The work of [IX] examined the propagation of a polarized Shear Horizontal (SH) wave in a self-reinforced cylinder enclosing a pre-stressed piezoelectric cylinder. It is presumed that the interaction of the two media is mechanically flawed. An analytical analysis of the mathematical formulation has been constructed to derive the dispersion relation. A seismic circular cylinder in a consistent, isotropic, linear medium was investigated in the study [XV] under the condition of an antiplane elastic wave concealing with a multilayer cloak with an imperfect interface. Spring modeling and the Ricker wavelet were used to depict the imperfect interface and transient seismic wave in the research [V]. The dynamic stress concentration factor for a plane SH-wave acting on an elliptical inclusion with defective interfaces was calculated using analytic methods using the Fourier transformation and the method of waveform expansion alternatively. The article [XII] presented findings from research into the transmission of SH waves via a cylindrical construction made up of thin layers of two materials with an unsatisfactory interface. Mechanical imperfections exist at the contact between the two materials. Analytical results for the distribution relations are obtained. Various (numerical) graphs are made to illustrate how variables such as rotation, beginning tension, and mechanically defective factors affect the phase velocity. The work [I] examined a dual

multiferroic composite that combines piezoelectric and ferromagnetic properties. An analytical approach is employed to examine the shear wave propagation in a PE-wrapped PM-unsatisfactory interfaced layered pre-stressed spinning cylindrical tube construction. There is a good chance that the interface in question has mechanical, electrical, and electrical damage. In their description of the imperfect contact, the researchers [VIII] used the spring model. To characterize the transient seismic wave, they used the Ricker wavelet. In the wave functional expansions approach and the Fourier transformation, an equation for the fluctuating concentration of stress factor was obtained for a circular inclusion in infinite space subjected to a plane SH wave, which includes faulty interfaces. The work [X] explored the transmission of torsion waves within a compound cylinder that has been pre-stressed on all three axes and has imperfect contact. To formulate the issue, they have used the piecewise homogeneous body model and a linearized version of the theory of elastic waves in three dimensions. The study assessed an analytical model that relies explicitly on both asymmetric and ax symmetric flaws. Twelve marine pressure hulls with ax symmetric flaws are subjected to nonlinear Finite Element Analysis (FEA) to explore the stress evolution and ultimately build such a model. Three collapse models are qualified using the insights from these experiments.

III. Formulation of the problem

A cylindrical arrangement with a finite width of concentric FAEM layers and an insufficiently connected Electrostrictive material cylinder is thought to be the mode of SAWP in an Electrostrictive layered structure. The FAEM cylindrical layer width, h (= r.$q_1 - q_2$), is found by calculating the cylindrical structure's inner and outer radii, represented as $q_1 - q_2$ and q_2, respectively. The cylindrical coordinate system's θ direction corresponds to wave propagation, while the z-axis is used to describe the cylinder and FAEM layer, which is composed of linearly transversely isotropic Electrostrictive material. The radial orientation of the cylinder is represented by the r-axis, and the structure's center appears as *P*. The Electrostrictive material's constitutive relations are defined as

$$\sigma_{ji} = d_{jilk}T_{lk} - f_{lji}F_l, \;\; C_i = f_{ilk}T_{lk} + \varepsilon_{il}E_l \tag{1}$$

The strain tensors, electric shift, electric field intensities, and stress tensors are denoted by σ_{ji}, T_{lk}, C_i, and E_l, respectively. The elastic, electrostrictive, and dielectric values are d_{jilk}, f_{ilk}, and ε_{il}, respectively. Considering Eq. (1), the Electrostrictive medium's constitutive equations may alternatively be expressed in cylindrical dimensions as

$$\begin{pmatrix}\sigma_{qq}\\ \sigma_{\theta\theta}\\ \sigma_{yy}\\ \sigma_{\theta y}\\ \sigma_{qy}\\ \sigma_{q\theta}\end{pmatrix} = \begin{pmatrix} d_{11} & d_{12} & d_{13} & 0 & 0 & 0\\ d_{12} & d_{11} & d_{13} & 0 & 0 & 0\\ d_{13} & d_{13} & d_{13} & 0 & 0 & 0\\ 0 & 0 & 0 & d_{44} & 0 & 0\\ 0 & 0 & 0 & 0 & d_{44} & 0\\ 0 & 0 & 0 & 0 & 0 & \frac{d_{11}-d_{12}}{2}\end{pmatrix}\begin{pmatrix}T_{qq}\\ T_{\theta\theta}\\ T_{yy}\\ T_{\theta y}\\ T_{qy}\\ T_{q\theta}\end{pmatrix} - \begin{pmatrix} 0 & 0 & f_{31}\\ 0 & 0 & f_{31}\\ 0 & 0 & f_{33}\\ 0 & f_{15} & 0\\ f_{15} & 0 & 0\\ 0 & 0 & 0\end{pmatrix}\begin{pmatrix}F_q\\ F_\theta\\ F_y\end{pmatrix} \tag{2}$$

$$\begin{pmatrix} C_q \\ C_\theta \\ C_y \end{pmatrix} = \begin{pmatrix} 0 & 0 & 0 & 0 & f_{15} & 0 \\ 0 & 0 & 0 & f_{15} & 0 & 0 \\ f_{31} & f_{31} & f_{33} & 0 & 0 & 0 \end{pmatrix} \begin{pmatrix} T_{qq} \\ T_{\theta\theta} \\ T_{yy} \\ T_{\theta y} \\ T_{qy} \\ T_{q\theta} \end{pmatrix} \begin{pmatrix} \varepsilon_{11} & 0 & 0 \\ 0 & \varepsilon_{11} & 0 \\ 0 & 0 & \varepsilon_{33} \end{pmatrix} \begin{pmatrix} F_q \\ F_\theta \\ F_y \end{pmatrix} \quad (3)$$

In this context, φ stands for the electric potential while$v$,u, and x are the mechanism of dislocation along the q, θ, and z axes, in that order, correspondingly.

$$T_{qq} = \frac{\partial v}{\partial q}, T_{q\theta} = \left[\frac{\partial u}{\partial q} - \frac{u}{q} + \frac{1}{q}\frac{\partial v}{\partial \theta}\right], T_{qy} = \left[\frac{\partial x}{\partial q} + \frac{\partial v}{\partial y}\right], T_{\theta\theta} = \frac{1}{q}\left[v + \frac{\partial u}{\partial \theta}\right]$$

$$T_{\theta y} = \left[\frac{1}{q}\frac{\partial x}{\partial \theta} + \frac{\partial u}{\partial y}\right], T_{yy} = \frac{\partial x}{\partial y}, F_q = -\frac{\partial \emptyset}{\partial q},\ F_\theta = -\frac{1}{q}\frac{\partial \emptyset}{\partial \theta}, F_y = -\frac{\partial \emptyset}{\partial y}, \quad (4)$$

When there is no external force acting on the body, the cylindrical coordinate system's Equation of motion, including stress components and the charge-free version of Gauss's law of electrostatics, states as

$$\frac{\partial \sigma_{qq}}{\partial q} + \frac{1}{q}\frac{\partial \sigma_{q\theta}}{\partial \theta} + \frac{\partial \sigma_{qy}}{\partial y} + \frac{\sigma_{qq} - \sigma_{\theta\theta}}{q} = \rho \frac{\partial^2 v}{\partial s^2} \quad (5)$$

$$\frac{\partial \sigma_{q\theta}}{\partial q} + \frac{1}{q}\frac{\partial \sigma_{\theta\theta}}{\partial \theta} + \frac{\partial \sigma_{\theta y}}{\partial y} + \frac{2\sigma_{q\theta}}{q} = \rho \frac{\partial^2 v}{\partial s^2} \quad (6)$$

$$\frac{\partial \sigma_{qy}}{\partial q} + \frac{1}{q}\frac{\partial \sigma_{\theta y}}{\partial \theta} + \frac{\partial \sigma_{yy}}{\partial y} + \frac{2\sigma_{qy}}{q} = \rho \frac{\partial^2 x}{\partial s^2} \quad (7)$$

$$\frac{\partial C_q}{\partial q} + \frac{1}{q}\frac{\partial C_\theta}{\partial \theta} + \frac{\partial C_y}{\partial y} + \frac{C_q}{q} = 0 \quad (8)$$

A material's mass density is represented by ρ. Presuming the SAWP travels in the θ-direction, we can describe the electric potential and mechanical displacements in the following way:

$$v = u = 0 \quad x = x(q, \theta, s), \quad \emptyset = \emptyset(q, \theta, s)\ and\ \frac{\partial ()}{\partial y} \equiv 0 \quad (9)$$

$$\sigma_{qy} = d_{44}\frac{\partial x}{\partial q} + f_{15}\frac{\partial \emptyset}{\partial q}. \quad \sigma_{\theta y} = \frac{1}{q}\left(d_{44}\frac{\partial x}{\partial \theta} + f_{15}\frac{\partial \emptyset}{\partial \theta}\right) \quad (10)$$

$$C_q = f_{15}\frac{\partial x}{\partial q} - \varepsilon_{11}\frac{\partial \emptyset}{\partial q}, \quad C_\theta = \frac{1}{q}\left(f_{15}\frac{\partial x}{\partial \theta} - \varepsilon_{11}\frac{\partial \emptyset}{\partial \theta}\right) \quad (11)$$

When equations (4) and (9) are substituted into equations (2) and (3), the following relations are obtained and Given Eq. (9)–(11), the motion equations (Eq. (5) and (6)) become zero, and Eq. (7) and (8) has the form as

$$d_{44}\nabla^2 x + f_{15}\nabla^2 \phi = \rho \frac{\partial^2 x}{\partial s^2} \quad (12)$$

$$f_{15}\nabla^2 x - \varepsilon_{11}\nabla^2 \phi = 0 \quad (13)$$

The polar coordinate version of the two-dimensional Laplace operator is denoted by$\nabla^2 = \frac{\partial}{two\partial q^2} + \frac{1}{q}\frac{\partial}{\partial q} + \frac{1}{q^2}\frac{\partial^2}{\partial \theta^2}$. It is possible to add functional guardedness into the FAEM layer by taking into account all of its material characteristics in the radial

dissimilarity as the layer $(q_1 < q \leq q_2)$ is functionally gradient and improves the Electrostrictive material's qualities.

$$d_{44} = d_{44}^{(E)}\left(\frac{q}{q_2}\right)^k, f_{15} = f_{15}^{(E)}\left(\frac{q}{q_2}\right)^k, \varepsilon_{11} = \varepsilon_{11}^{(E)}\left(\frac{q}{q_2}\right)^k, \tag{14}$$

This is where$\varepsilon_{11}, f_{15}, d_{44},$ and ρ represent the SAWP elastic modulus, mass density dielectric values, and Electrostrictive constant of the FAEM layer, respectively. At$q = q_2$, the corresponding values are $d_{44}^{(E)}$, $f_{15}^{(E)}\left(\frac{q}{q_2}\right)^k$, $\varepsilon_{11}^{(E)}$, and $\rho(E)$, and k is the undefined useful gradient parameter. Under the above assumptions, the electric potential and displacing elements for a FAEM layer $(q_1 < q \leq q_2)$ may be expressed as $x^{(E)}, \phi^{(E)}$, respectively, using equations (12) and (13) and Eq. (14).

$$d_{44}^{(E)}\left[q^2\frac{\partial^2 x^{(E)}}{\partial q^2} + q(k+1)\frac{\partial x^{(E)}}{\partial q} + \frac{\partial^2 x^{(E)}}{\partial \theta^2}\right] + f_{15}^{(E)}\left[q^2\frac{\partial^2 \phi^{(E)}}{\partial q^2} + q(k+1)\frac{\partial \phi^{(E)}}{\partial q} + \frac{\partial^2 \phi^{(E)}}{\partial \theta^2}\right] = \frac{q^2}{\rho^{(E)}}\frac{\partial^2 x^{(E)}}{\partial s^2} \tag{15}$$

$$f_{15}^{(E)}\left[q^2\frac{\partial^2 x^{(E)}}{\partial q^2} + q(k+1)\frac{\partial x^{(E)}}{\partial q} + \frac{\partial^2 x^{(E)}}{\partial \theta^2}\right] - \varepsilon_{11}^{(E)}\left[q^2\frac{\partial^2 \phi^{(E)}}{\partial q^2} + q(k+1)\frac{\partial \phi^{(E)}}{\partial q} + \frac{\partial^2 \phi^{(E)}}{\partial \theta^2}\right] = 0 \tag{16}$$

By modifying Equations (15) and (16), we get these field calculations for mechanical shifting and the electrical potential functions. The field calculations of mechanical displacement and the electric potential component will be used in (17) and (18) as

$$q^2\frac{\partial^2 x^{(E)}}{\partial q^2} + q(k+1)\frac{\partial x^{(E)}}{\partial q} + \frac{\partial^2 x^{(E)}}{\partial \theta^2} = \frac{q^2}{\beta_1^2}\frac{\partial^2 x^{(E)}}{\partial s^2} \tag{17}$$

$$q^2\frac{\partial^2 \phi^{(E)}}{\partial q^2} + q(k+1)\frac{\partial \phi^{(E)}}{\partial q} + \frac{\partial^2 \phi^{(E)}}{\partial \theta^2} = \frac{f_{15}^{(E)} q^2}{\varepsilon_{11}^{(E)}\beta_1^2}\frac{\partial^2 x^{(E)}}{\partial s^2} \tag{18}$$

$$\beta_1 = \sqrt{\frac{\bar{d}_{44}}{\rho^{(E)}}} \; and \; \bar{d}_{44} = \bar{d}_{44}^{(E)} + \frac{\left(f_{15}^{(E)}\right)^2}{\varepsilon_{11}^{(E)}}$$

To simplify things and show that the material constants have a superscript (o), we can write the field equations of the Electrostrictive cylinder as $D_{44}^{(O)}$, $F_{15}^{(O)}, \varepsilon_{11}^{(O)}, \rho^{(O)}$, $X^{(O)}$ and $\phi^{(O)}$ $(0 < q \leq q_1)$ for the range of values of q from $(0 < q \leq q_1)$, and for the electric potential as$\phi^{(O)}$. Eq (12) Also, by lowering to (13)

$$q^2\frac{\partial^2 x^{(O)}}{\partial q^2} + q\frac{\partial x^{(O)}}{\partial q} + \frac{\partial^2 x^{(O)}}{\partial \theta^2} = \frac{q^2}{\beta_2^2}\frac{\partial^2 x^{(O)}}{\partial s^2} \tag{19}$$

$$q^2\frac{\partial^2 \phi^{(O)}}{\partial q^2} + q\frac{\partial \phi^{(O)}}{\partial q} + \frac{\partial^2 \phi^{(O)}}{\partial \theta^2} = \frac{q^2 f_{15}^{(O)}}{\beta_2^2 \varepsilon_{11}^{(O)}}\frac{\partial^2 x^{(O)}}{\partial s^2} \tag{20}$$

$$\beta_2 = \sqrt{\frac{\bar{d}_{44}}{\rho^{(O)}}}\ and\ \bar{d}_{44} = \bar{d}_{44}^{(O)} + \frac{\left(f_{15}^{(O)}\right)^2}{\varepsilon_{11}^{(O)}}$$

The FAEM layer's outer surface ($q>q_2$) is in the air, which has a much lower dielectric constant ($\varepsilon 0$) than the Electrostrictive medium. Hence, air may be considered a vacuum, and the electric potential φ0 according to the Laplacian Equation.

The FAEM layer's outer surface ($q>q_2$) is in air, which has a much lower dielectric constant ($\varepsilon 0$)than the Electrostrictive medium. Hence, air may be considered a vacuum, and the electric potential φ0 according to the Laplacian Equation. Vacuum quantities are denoted by the subscript 0.

$$\nabla^2\phi_0 = 0 \tag{21}$$

IV. Solution of the problem

The electric potentials of the vacuum, the FGPM layer, and the Electrostrictive cylinder were calculated together with the displacement components using Eq. (17)–(21). Given that the shear acoustic wave is moving continuously in a circumferential direction, and given that the solutions to equations (17) and (18) are given by the formulation

$$x^{(E)}(q,\theta,s) = X^{(E)}(q)\cos(m\theta - \omega s)\, q^{-k/2} \tag{22}$$

$$\phi^{(E)}(q,\theta,s) = \varphi^{(E)}(q)\cos(m\theta - \omega s) q^{-k/2} \tag{23}$$

Where m is a real integer, and $X^{(E)}(q)\varphi^{(E)}(q)\ m$ is an unidentified function. Given Eq (22) and (23), Eqs. (17) And (18) result in

$$q^2\frac{d^2X^{(E)}(q)}{dq^2} + q\frac{dX^{(E)}(q)}{dq} + \left[\frac{q^2\omega^2}{\beta_1^2} - \left(m^2 + \frac{k^2}{4}\right)\right]X^{(E)}(q) = 0 \tag{24}$$

and

$$q^2\frac{d^2\varphi^{(E)}(q)}{dq^2} + q\frac{d\varphi^{(E)}(q)}{dq} - \left(m^2 + \frac{k^2}{4}\right)\varphi^{(E)}(q) = \frac{f_{15}^{(E)}}{\varepsilon_{11}^{(E)}}\left[q^2\frac{d^2X^{(E)}(q)}{dq^2} + q\frac{dX^{(E)}(q)}{dq} - \left(m^2 + \frac{k^2}{4}\right)W^{(E)}(q)\right] \tag{25}$$

The solution to Equation (24) is provided by, and it takes the structure of Bessel's disparity calculation of arrange$o\left(=\sqrt{m^2 + \frac{k^2}{4}}\right)$

$$X^{(E)}(q) = D_1 I_o\left(\frac{\omega q}{\beta_1}\right) + D_2 Z_o\left(\frac{\omega q}{\beta_1}\right) \tag{26}$$

The first type of Bessel's function of O^{th}order is denoted by Zo (·), and the second kind is denoted by $I_o(\cdot)$, $\mathrm{Z_o}(\cdot)$, whereas $D_1\ and\ D_2$ are constants that cannot be calculated. Looking at Eq. (26), we may express the solution of Eq. (25) as

$$\varphi^{(E)}(q) = D_1^* q^{-o} + D_2^* q^{-o} + \frac{f_{15}^{(E)}}{\varepsilon_{11}^{(E)}}\left(D_1 I_o\left(\frac{\omega q}{\beta_1}\right) + D_2 Z_o\left(\frac{\omega q}{\beta_1}\right)\right) \tag{27}$$

The values of $D_1\ and\ D_2$ are unknown. The following is the Equation for the electric potential and displacement component of a layer of FAEM ($q_1 < q \le q_2$)

$$x^{(E)} = \left[D_1 I_o\left(\frac{\omega q}{\beta_1}\right) + D_2 Z_o\left(\frac{\omega q}{\beta_1}\right)\right] q^{-k/2}\cos\left(m\theta - \omega s\right) \tag{28}$$

$$\phi^{(E)} = \left[D_1^* q^{-o} + D_2^* q^{o} + \frac{f_{15}^{(E)}}{\varepsilon_{11}^{(E)}}\left(D_1 I_o\left(\frac{\omega q}{\beta_1}\right) + D_2 Z_o\left(\frac{\omega q}{\beta_1}\right)\right)\right] q^{-\frac{k}{2}\cos(m\theta-\omega s)} \tag{29}$$

In the same way, the electric potential and displacement component of the Electrostrictive cylinder $(0 < q \leq q_1)$will be described as

$$x^{(O)} = \left[C_1 I_m\left(\frac{\omega q}{\beta_2}\right) + C_2 Z_m\left(\frac{\omega q}{\beta_2}\right)\right]\cos(m\theta - \omega s) \tag{30}$$

$$\phi^{(O)} = \left[C_1^* q^{-m} + D_2^* q^{m} + \frac{f_{15}^{(O)}}{\varepsilon_{11}^{(O)}}\left(C_1 I_m\left(\frac{\omega q}{\beta_2}\right) + C_2 Z_m\left(\frac{\omega q}{\beta_2}\right)\right)\right]\cos(m\theta - \omega s) \tag{31}$$

The variables $C_1, C2, and\ C_1^* C_2^*$ are constants that cannot be determined, whereas the functions $I_m(\cdot)\mathrm{Z_m}(\cdot)$are the first and second kinds of nth-order Bessel's functions, respectively. Applying the situation at the cylinder's border (Eq. (44)), the Electrostrictive electric potential and hydraulic displacement $(0 < q \leq \mathrm{q_1})$ lead to

$$x^{(O)} = C_1 I_m\left(\frac{\omega q}{\beta_2}\right)\cos\left(m\theta - \omega s\right) \tag{32}$$

$$\phi^{(O)} = \left[C_1^* q^{-m} + \frac{f_{15}^{(O)}}{\varepsilon_{11}^{(O)}} C_1 I_m\left(\frac{\omega q}{\beta_2}\right)\right]\cos\left(m\theta - \omega s\right) \tag{33}$$

To get the electric potential in a vacuum, we may use the following Equation as a starting point:

$$\phi_0 = \varphi_0(q)\cos\left(m\theta - \omega s\right) \tag{34}$$

The indeterminate function is represented by $\varphi_0(q)$. The electric potential of a vacuum can be determined by plugging into Eq. (21) and keeping in mind that the electric potential of a vacuum tends to zero as q.

$$\phi_0 = B_0 q^{-m}\cos\left(m\theta - \omega s\right) \tag{35}$$

Here$B_0$is the undetermined constant.

V. Boundary conditions

There are two types of boundary conditions applied to the outside of the FAEM cylindrical layer (i.e., q=q_2): an electrical short condition and an electrical open condition. This surface is mechanically traction-free. The following equations may be used to represent these boundaries mathematically: The open area of the FAEM layer, which is typical in both open and short examples, is mechanically traction-free, as shown by

$$\sigma_{qy}^{(E)} = 0 \quad q = q_2 \tag{36}$$

When the FAEM layer is free-surfaced, the electrically short situation is given by

$$\phi^{(E)} = 0 \quad q = q_2 \tag{37}$$

The state of electrical openness at the FAEM layer's surface that is free is defined as

$$\phi^{(E)} = \phi_0 \quad q = q_2 \tag{38}$$

and

$$C_q^{(E)} = -\varepsilon_0 \frac{\partial \phi_0}{\partial q} \quad q = q_2 \tag{39}$$

It is presumed that the electrical and mechanical interaction (i.e.,$q = q_2$) between the Electrostrictive cylinder and the FAEM layer becomes defective due to damage. An incomplete interfacial model satisfies the following relations: although pressures and electrical shifts are regular, mechanical shifts and electricity potentials are jumped over the interface.

$$\sigma_{qy}^{(E)} = \alpha_1\left(x^{(E)} - x^{(O)}\right) \quad q = q_1 \tag{40}$$

$$C_q^{(E)} = -\propto_2 \left(\phi^{(E)} - \phi^{(O)}\right) \quad q = q_1 \tag{41}$$

$$\sigma_{qy}^{(E)} = \sigma_{qy}^{(O)} \quad q = q_1 \tag{42}$$

$$C_q^{(E)} = C_q^{(O)} \quad q = q_1 \tag{43}$$

The FAEM layer and the Electrostrictive cylinder are represented by superscripts (E) and (O), respectively, in the stresses and electric displacement components. The two non-negative, consistent parameters $\alpha\alpha_1 \ and \ \alpha_2$ that describe the imperfect interface are constants. It is clear that the contact is mechanically and/or dielectrically defective unless $\alpha_1 \longrightarrow \infty$and $\propto_2 \longrightarrow \infty$ are both infinite. By the time the Electrostrictive cylinder reaches its origin, the mechanical shift and potential for electricity will have become limited.

$$q \longrightarrow 0, \ \ x^{(O)}\phi^{(O)} \longrightarrow finite \ value \tag{44}$$

V.i. Special Case

When the FAEM layer and Electrostrictive cylinder are fully bonded, homogenous, and isotropically elastic, i.e., $f = 0, a_{15}^{(L)} = a_{15}^{(B)} = \varepsilon_{11}^{(L)} = \varepsilon_{11}^{(B)} = 0, \alpha_1 \to \infty, \alpha_2 \to \infty \ and \ v_{44}^{(L)} = \mu_1, v_{44}^{(B)}\mu_2andv_{44}^{(L)} = \mu_1, v_{44}^{(B)}\mu_2$, such that in the circumstances of an electrical short and an electrical open,

$$\tan\left(rz\sqrt{\frac{v^2}{\beta_1^{2-1}}}\right) = \frac{\mu_2\sqrt{1-\frac{v^2}{\beta_2^2}}}{\mu_1\sqrt{\frac{v^2}{\beta_1^2}-1}}, \tag{45}$$

This is the Equation for the classical Love wave

Table 1 : Materials constants used for imperfect cylinders

Material	Material constants			Density
	$v_{44}(10^9\,N/m^2$	$a_{15}(C/m^2)$	$\varepsilon_{11}(10^{-9}\,C^2/Nm^2$	$\rho(10^3 kg/m^3)$
AIN	119.0	-0.49	10.0	4.512
PZT-5H	23.0	18.00	28.7	7.600

VI. Numerical Result and Discussion

To illustrate the analytical results for the SAWP in an Electrostrictive cylindrical structure, this section employs numerical modeling in conjunction with graphical presentation. A cylinder of Electrostrictive material for imperfect bonding and a layer of concentric FAEM cylindrical components make up the construction. For the inner Electrostrictive material cylinder, PZT-5H is used, and for the FAEM cylindrical layer, AlN. In a vacuum, a dielectric parameter ($\varepsilon 0$) is 8.85 × 10−12 $C/Nm2$. When it comes to computing, the features of mechanical and electrical imperfections are specified as follows

$$R_1 = \frac{\propto_1 q_1}{(f_{15}^{(E)})^2 \Big/ \varepsilon_{11}^{(E)}}\,, \tag{46}$$

$$R_2 = \frac{\propto_2 q_2}{\varepsilon_{11}^{(E)}} \tag{47}$$

Under both Electrically Short Conditions (ESC) and Electrically Open Conditions (EOC), Figures 1 and 2 demonstrate the relationship between the undefined wave number (rz), the investigated Electrostrictive cylindrical structure, and the undefined phase velocity (PV) of SAWP as a function of the useful gradient parameter (l).

VI.i. Phase velocity and the functional gradient parameter

An Electrostrictive cylindrical structure's PV of SAWP is shown in Figure 1 to be significantly affected by the Functional Gradient Parameter (FGP) linked to the FAEM layer. The second and third curves show the effects of the GP on the FAEM layer, whereas 1st curve is obtained by considering the FAEM layer as an Electrostrictive homogenous layer. SAWP velocities in an Electrostrictive cylindrical structure under ESC and EOC are shown in Figures 1a and 1b, respectively, as an FGP. While the EOC shows that the gradient parameter has a reducing influence on PV, the ESC modifies PV. Also, looking at Figures 1a and 1b side by side, we can see that the gradient parameter has a bigger impact on the ESC state compared to the EOC.

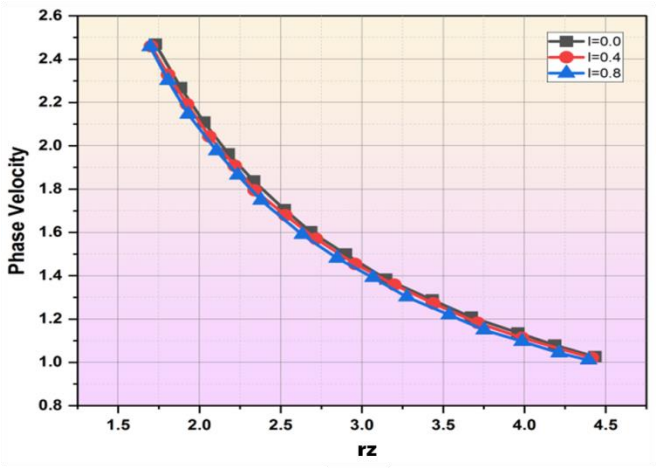

(a) ES

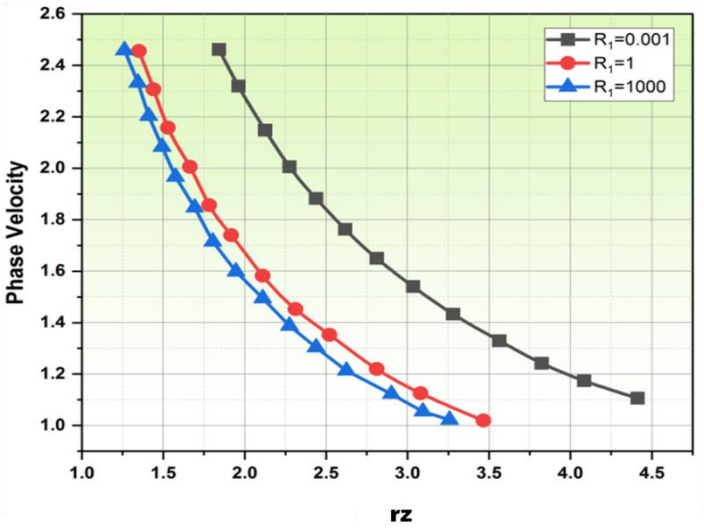

(b) EOC

Fig. 1. a) ES and b) EOC explore the influence of the FGP(l)connected with the FAEM layer without dimensions PV ($c/\beta 1$) of SAWP as a function of dimensionless wave number (rz).

VI.ii. Imperfection parameter's impact on phase velocity

Regarding the incorrect connection of the FAEM and Electrostrictive cylinder, two figures illustrate the impact of the mechanical imperfection parameter (R1) and the electrical imperfection parameter (EIP) on the PV of a SAWP, respectively. Until the imperfection parameters reach very high values or approach infinity, the interface's mechanical or electrical imperfection is substantial. After this point, a full connection is formed, permitting conduction. The degree of imperfection between surfaces is proportional to the Mechanical Imperfection Parameter (MIP). Figure 1 shows a very imperfect contact, Figure 2 a slightly imperfect interface, and Figure 3 a completely

bonded or conducting interface, all shown by their respective Dispersion Curves. The impact of the MIP on the SAWP's PV may be seen in Figures 2a for ESC and Figure 2b for open circumstances. Because the MIP has a constructive impact on the PV under ESC and EOC, it reaches its maximum when the contract is fully bonded. The mechanical defect parameter is more noticeable in the ESC compared to the EOC, according to a comparison of Figures 2a and b.

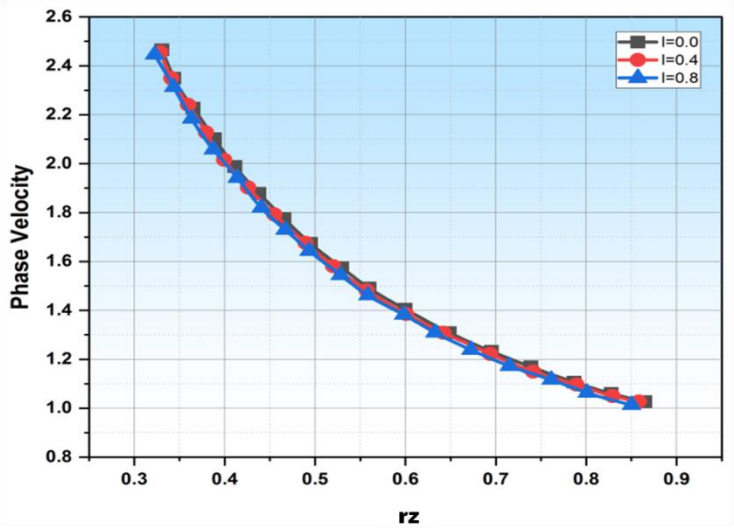

a) ESC

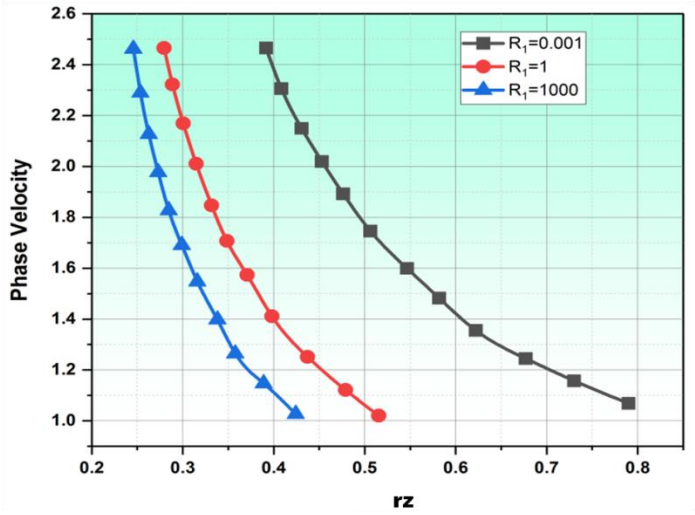

b) EOC

Fig. 2. The impact of inadequate bonding between the layer and cylinder interface, represented by the MIP (R1), on the undefined PV (c/β1) of SAWP under two conditions: Undefined wave number (rz) values are the main focus of the following: a) ESC and b) EOC

Figure 3a shows the effect of an electrically short state on the PV of an SAWP, and Figure 3b shows the effect of an EOC. When the EIP values grow, the SAWP's phase velocity drops under ESC, while it positively affects the shear acoustic wave's phase velocity under EOC.

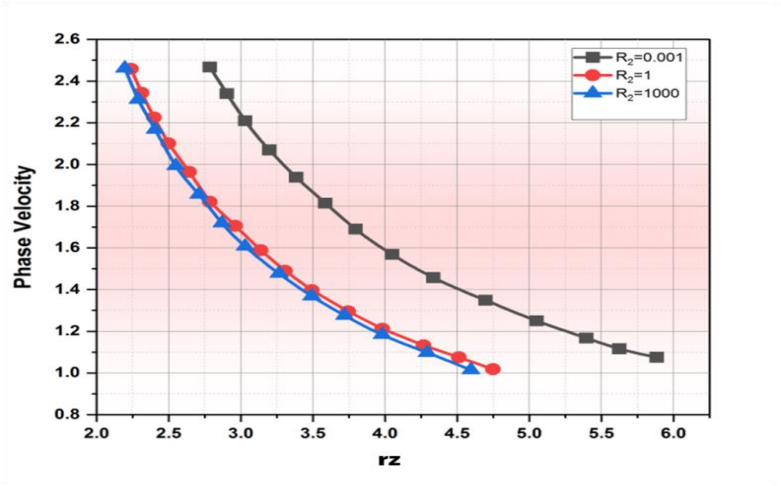

a) ES

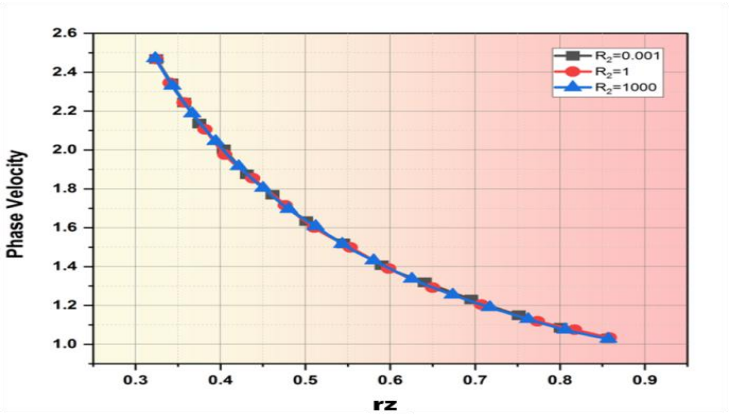

b) EOC

Figure 3: Explore the influence of the EIP (R2) at the inadequately bonded layer-cylinder interface on the dimensionless PV (c/β1) of SAWP about the dimensionless wave number (rz) under two conditions: a) ES and b) EOC.

VII. Conclusion

Our investigation into the characteristics of shear wave propagation in Electrostrictive materials, especially in the context of an imperfect cylinder, has shed important light on the complex dynamics of these intelligent materials. We now have a better knowledge of how electrical stimuli and external pressures, particularly when geometric flaws are present, affect Electrostrictive materials thanks to a mix of theoretical analysis, numerical simulations, and experimental studies. Our functional analysis has brought to light the complex interactions between the intrinsic

characteristics of Electrostrictive materials and the difficulties posed by the cylindrical structure's flaws. The results indicate that the particular geometry and flaws in the structure, along with the material's Electrostrictive response, have a major impact on the shear wave propagation behavior. The future potential applications of wave propagation in defective cylindrical materials are enormous. With the development of technology, researchers seek to more accurately characterize and comprehend the behavior of waves in these materials. More accurate modeling and study of wave propagation events are probably going to be made possible by improved computer techniques and sophisticated imaging technology. This might result in advances in material science applications, structural health monitoring, and non-destructive testing.

Conflict of Interest:

There are no conflict of interest regarding this paper.

Reference

I. Chaudhary, S., Sahu, S.A., Singhal, A. and Nirwal, S., 2019. Interfacial imperfection study in a pres-stressed rotating multiferroic cylindrical tube with wave vibration analytical approach. *Materials Research Express*, *6*(10), p.105704.

II. Della Schiava, N., Thetpraphi, K., Le, M.Q., Lermusiaux, P., Millon, A., Capsal, J.F. and Cottinet, P.J., 2018. Enhanced figures of merit for a high-performing actuator in electrostrictive materials. *Polymers*, *10*(3), p.263.

III. Di Stefano, S., Miller, L., Grillo, A. and Penta, R., 2020. Effective balance equations for electrostrictive composites. *Zeitschrift für angewandte Mathematik und Physik*, *71*, pp.1-36.

IV. Liang, C., Yaw, Z. and Lim, C.W., 2023. Thermal strain energy induced wave propagation for imperfect FGM sandwich cylindrical shells. *Composite Structures*, *303*, p.116295.

V. Luo, H., Tao, M., Wu, C. and Cao, W., 2023. Dynamic response of an elliptic cylinder inclusion with imperfect interfaces subjected to plane SH wave. *Geomechanics and Geophysics for Geo-Energy and Geo-Resources*, *9*(1), p.24.

VI. Manduca, A., Bayly, P.V., Ehman, R.L., Kolipaka, A., Royston, T.J., Sack, I., Sinkus, R. and Van Beers, B.E., 2021. MR elastography: Principles, guidelines, and terminology. *Magnetic resonance in medicine*, *85*(5), pp.2377-2390.

VII. Marino, A., Genchi, G.G., Sinibaldi, E. and Ciofani, G., 2017. Piezoelectric effects of materials on bio-interfaces. *ACS Applied Materials & interfaces*, *9*(21), pp.17663-17680.

VIII. Ming, T., Hao, L., Rui, Z. and Gongliang, X., 2023. *Dynamic response of an elliptic cylinder inclusion with imperfect interfaces subjected to plane SH wave* (No. EGU23-7726). Copernicus Meetings.

IX. Pankaj, K.K., Sahu, S.A. and Kumari, S., 2020. Surface wave transference in a piezoelectric cylinder coated with reinforced material. *Applied Mathematics and Mechanics*, *41*, pp.123-138.

X. Reijmers, J.J., Kaminski, M.L. and Stapersma, D., 2022. Analytical formulations and comparison of collapse models for risk analysis of axisymmetrically imperfect ring-stiffened cylinders under hydrostatic pressure. *Marine Structures*, *83*, p.103161.

XI. Ryu, J. and Jeong, W.K., 2017. Current status of musculoskeletal application of shear wave elastography. *Ultrasonography*, *36*(3), p.185.

XII. Singhal, A., Baroi, J., Sultana, M. and Baby, R., 2022. Analysis of SH-waves propagating in multiferroic structure with interfacial imperfection. *Mechanics Of Advanced Composite Structures*, *9*(1), pp.1-10.

XIII. Trujillo, D.P., Gurung, A., Yu, J., Nayak, S.K., Alpay, S.P. and Janolin, P.E., 2022. Data-driven methods for discovery of next-generation electrostrictive materials. npj *Computational Materials*, 8(1), p.251.

XIV. Uchino, K., 2017. The development of piezoelectric materials and the new perspective. In *Advanced Piezoelectric Materials* (pp. 1-92). Woodhead Publishing.

XV. Wijeyewickrema, A.C. and Leungvichcharoen, S., 2022. Effect of imperfect contact on the cloaking of a circular elastic cylinder from antiplane elastic waves. *Mechanics Research Communications*, *124*, p.103964.